

Load-Induced Hydrodynamic Lubrication of Porous Films

Tushar Khosla,[†] Joseph Cremaldi,[†] Jeffrey S. Erickson,[‡] and Noshir S. Pesika^{*,†}

[†]Department of Chemical and Biomolecular Engineering, Tulane University, 6823 St. Charles Avenue, New Orleans, Louisiana 70118, United States

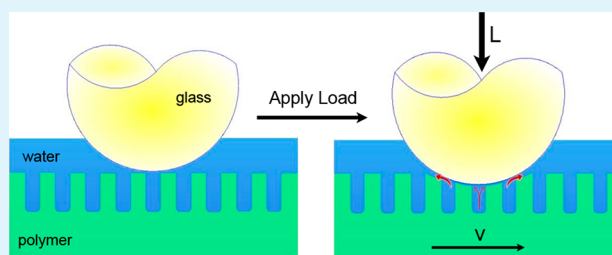
[‡]Center for Bio/molecular Science and Engineering, Naval Research Lab, Washington, D.C. 20375, United States

S Supporting Information

ABSTRACT: We present an exploratory study of the tribological properties and mechanisms of porous polymer surfaces under applied loads in aqueous media. We show how it is possible to change the lubrication regime from boundary lubrication to hydrodynamic lubrication even at relatively low shearing velocities by the addition of vertical pores to a compliant polymer. It is hypothesized that the compressed, pressurized liquid in the pores produces a repulsive hydrodynamic force as it extrudes from the pores. The presence of the fluid between two shearing surfaces results in low coefficients of friction ($\mu \approx 0.31$).

The coefficient of friction is reduced further by using a boundary lubricant. The tribological properties are studied for a range of applied loads and shear velocities to demonstrate the potential applications of such materials in total joint replacement devices.

KEYWORDS: lubrication, biomimetic, surface structure, friction, cartilage, aqueous lubricant



Lubricants play an integral role in the operation of several technologies, including internal combustion engines, vehicles, gear systems, compressors, turbines, and hydraulics, in addition to smaller scale technologies, including the lubrication of hard disk drives¹ and microelectromechanical systems (MEMs).² The main purposes of a lubricant are to reduce friction and material wear. Typically, to reduce the friction between surfaces, a liquid medium (e.g., oils containing additives or synovial fluid in joints) is used, which prevents two shearing surfaces from coming into intimate contact with each other thereby reducing interactions (such as van der Waals forces). Tribological studies include studies of the lubricating liquid,³ solid–liquid interaction,⁴ and surface engineering.⁵ Although a lot of research has gone into developing superior lubricants, relatively less research has gone into engineering surfaces, which exhibit low friction.

The coefficient of friction (COF) μ , defined by Amontons' Law⁶ as the ratio of the frictional force (F_x) to the normal load (L)

$$\mu = \frac{F_x}{L} \quad (1)$$

is typically used as a means of comparing the performance of different lubricant formulations. A low value of μ is desirable because this translates into low friction forces at a particular applied load L .

Friction between two molecularly smooth surfaces is caused by interfacial interactions (van der Waals attractive forces) within the contact zone.⁷ The Stribeck curve describes the various lubrication regimes⁸ as a function of the lubrication parameter $\eta V/P$ where η is the dynamic viscosity, V is the shear velocity, and P is the applied load. Considering a Newtonian

liquid and constant load the lubrication parameter is directly proportional to shear velocity. At low speeds, and in the absence of lubricant, the shearing surfaces come into intimate contact leading to large friction forces. In the boundary lubrication zone, a thin layer of lubricant, e.g., oil, exists between the two sliding surfaces. This decreases the Hamaker constant⁹ and increases surface separation¹⁰ resulting in lower van der Waals attractive forces and lower friction. It is important that the thickness of the lubricant is greater than surface asperities of the shearing surface.¹¹ As the surface shears, the boundary lubricant has to be continuously replaced. At high shear velocity, the sliding surfaces enter the hydrodynamic lubrication regime. In this regime, a thicker, pressurized layer of liquid exist between the shearing surfaces,¹² which provides lower friction. In addition, the two sliding surfaces are never in contact thereby reducing surface wear.

In this communication, we demonstrate how by engineering the design on a compliant polymer surface (i.e., adding vertical hollow pores), hydrodynamic lubrication can be exploited, even at low shear velocities where one would typically expect boundary lubrication to dominate for a flat surface. The idea is inspired by the lubrication mechanism of cartilage.^{13–17} Cartilage is a connective tissue found in many areas of the body including the joint between bones.¹⁸ It is composed of water (60–80%), collagen, and a small volume of cells (chondrocytes).¹⁹ Although there is still debate about the microstructure of collagen, it is agreed that the cartilage has an

Received: June 11, 2015

Accepted: July 29, 2015

Published: July 29, 2015



array of open and parallel tubular pores in axial and lateral directions.^{20,21} The cartilage is surrounded by an extracellular fluid, called synovial fluid.²² The synovial fluid runs through the pores of cartilage providing nutrition to the cells. The cartilage has a low coefficient of friction of 0.005–0.04.²³ The cartilage and synovial fluid works synergistically to make joint lubrication efficient. The load that is applied on the cartilage is supported by the extracellular matrix, which due to the charged species creates an osmotic pressure to hydrate the cartilage.²⁴ During movement, at high shear velocities, hydrodynamic lubrication regime dominates. It has been shown that the measured friction forces in the cartilage is inversely proportional to the pressure of the interstitial fluid.²⁵ The flow of interstitial fluid is regulated by the pore matrix.²⁶ It is believed that a thick pressurized layer of synovial fluid separates the shearing cartilage surface responsible for ultralow friction. Synovial fluid is rich in boundary lubricants: hyaluronic acid, surface active phospholipids, and superficial zone proteins.²⁷ These lubricants act as a sacrificial layer during shear at slow speeds, thus they need to be replaced continuously. Therefore, to successfully replicate such a system, it is important to consider both the properties of the lubricant and the surface mechanical and structural properties.

Various patterns (i.e., pore size and spacing) of porous polymer samples were created using polydimethylsiloxane (PDMS) to demonstrate the potential of reducing friction against other shearing surfaces through a load-induced hydrodynamic lubrication mechanism. PDMS is selected as a candidate material because it is stable in aqueous media, biocompatible and has a compressive modulus similar to that reported for cartilage (0.8–2 MPa). In a typical experiment, a fixed preload was applied on the polymer sample using CETR Universal Materials Tester and the friction force between the polymer sample and a spherical glass probe was measured while shearing a fixed distance at a constant speed. Similar to the “weeping” lubrication mechanism of the cartilage,^{11–16} the pressurized liquid supports most of the load, resulting in significant reduction in friction as shown schematically in Figure 1.

The coefficient of friction of PDMS and the glass probe by applying a 49 mN (5g) load were compared by shearing at a constant speed of 100 $\mu\text{m/s}$ under four test conditions: (1) flat PDMS and a glass lens under dry conditions; (2) flat PDMS and a glass lens under aqueous conditions; (3) porous PDMS and glass lens under dry conditions, and (4) porous PDMS (with various diameters and pore spacing) and glass lens under aqueous conditions. The glass probe and all samples were cleaned using air plasma for 60 s. Plasma treatment makes PDMS hydrophilic²⁸ and facilitates water to penetrate the pores of the porous surfaces. Each set of experiments was performed five times. The average coefficient of friction in each case is shown in Figure 2B.

The first set of experiments consisted of shearing a spherical silica surface against a flat PDMS surface under dry conditions. The Young's modulus of the PDMS surface is 1–2 MPa,²⁹ which allows for relatively large deformations upon application of a small normal load. The resulting large contact area and the fact that both surfaces have a high surface energy (due to plasma treatment) is consistent with the high coefficient of friction of around 3.68. Under aqueous conditions, water can act as a boundary lubricant. This effect is visible in the second sample set as the friction coefficient is reduced slightly from 3.7 to 3.16.

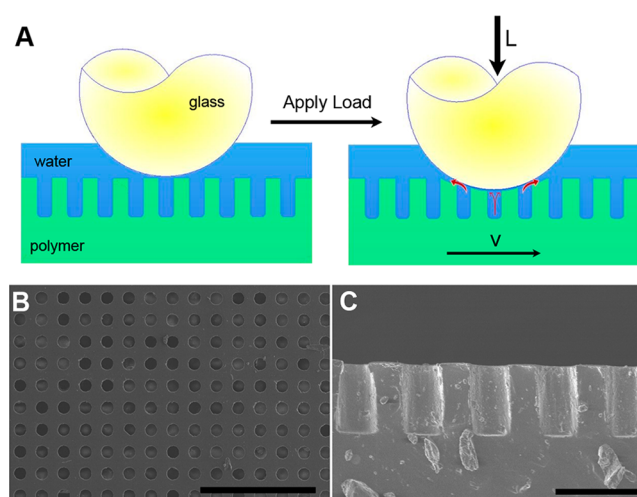


Figure 1. (A) Schematic illustration of the mechanism by which a thin fluid layer forms between a spherical glass surface and a porous polymer surface under an applied load. The thin film remains as the glass probe is sheared over the polymer surface at a constant velocity V . (B) Top-view SEM image of a porous polymer surface. Scale bar = 200 μm . (C) Cross-sectional side view of a porous polymer surface. Scale bar = 50 μm .

The modified Amontons' law,³⁰

$$F_x = \mu L + \Gamma A \quad (2)$$

where Γ is the shear stress and A is the true area of contact, explains the decrease in friction coefficient of patterned PDMS samples to 2.25 in sample set 3. Introduction of pores on the surface reduces the actual amount of polymer in contact with the probe thereby reducing the apparent (and true) area of contact between the two sliding surfaces. The drastic decrease in the coefficient of friction to a value of 0.31 under the aqueous conditions in patterned PDMS cannot be explained solely due to the boundary lubrication contribution of water. We hypothesize that as the silica probe (under an applied load) shears against the porous PDMS surface, water is extruded from the pores, resulting in a repulsive hydrodynamic force as the water drains. The draining water maintains a separation gap between the silica and porous PDMS surfaces, which changes the lubrication mechanism from boundary lubrication to hydrodynamic (or mixed) lubrication. As the probe moves, the pores on the trailing side no longer experience a compressive local stress and therefore elastically regain their original shape and water goes back in the pores. This mechanism ensures that the samples have low friction coefficient for an extended period of time as long as water is present.

To show that hydrodynamic lubrication can be exploited over a range of velocities, a PDMS sample, which had pores that were 40 μm deep, 20 μm in diameter, and spaced 20 μm apart (end to end), was tested over speeds ranging from 5 to 1000 $\mu\text{m/s}$ under aqueous conditions. The same PDMS sample was used to study the effect of increasing load on the coefficient of friction in aqueous conditions by increasing the load from 49 mN (5g) to 392 mN (40g). Figure 3 summarizes the results of both these test conditions.

It can be seen that the friction coefficient is low for the entire range of shear velocities. With respect to the influence of applied load, a slight decrease in the coefficient of friction is observed (from 0.28 to 0.26) with increasing loads. This

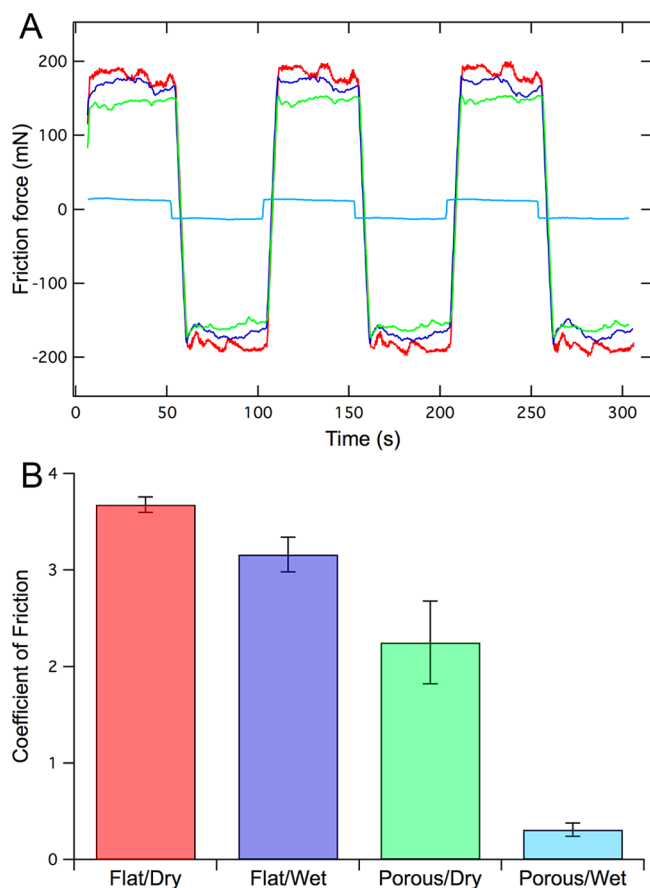


Figure 2. (A) Plot of a typical friction force vs time while shearing a glass probe on a PDMS surface for various test conditions: PDMS under dry conditions (red, sample set 1), flat PDMS with water (blue, sample set 2), textured PDMS under dry conditions (green, sample set 3) and textured PDMS under water (light blue, sample set 4). (B) Plot of the average coefficient of friction between a spherical glass probe and the polymer surface under various conditions. The applied load in all cases was 49 mN and the shearing speed was $100 \mu\text{m/s}$.

decrease in friction is small and is more significant at lower loads. It is proposed that this reduction in friction may be attributed to the fact that PDMS is compliant and therefore more pores can contribute as load is increased due to an increase in contact area. However, more controlled experiments are needed to confirm this trend; nevertheless, these results demonstrate that the system is robust and provides low friction over a wide range of shear velocities and applied loads.

So far, we have only mimicked the porous structure of cartilage. The coefficient of friction, although lower than a flat sample under similar conditions, is still much higher than cartilage. To further reduce friction, we used sodium dodecyl sulfate (SDS) as a boundary lubricant. Figure 4 shows the effects of using various concentrations of SDS for both flat and textured polymer samples.

It can be seen that SDS at a very small concentration of 1 mM acts as a boundary lubricant for a flat surface, but has no significant effect on the textured surface. The latter is not surprising since the flat surface produces a larger contact area and therefore boundary lubricants are expected to have a larger effect. However, by increasing the concentration of SDS we can see the contribution of the boundary lubricant even in the textured samples, presumably reducing friction at regions where

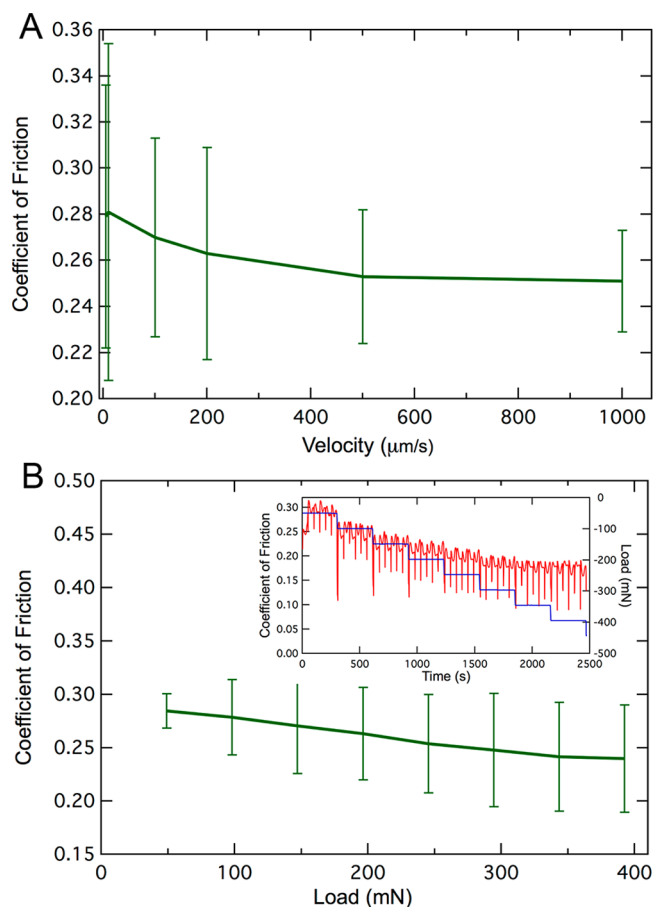


Figure 3. Plot of the coefficient of friction between a spherical glass probe and a porous PDMS surface as a function of (A) shear velocity, and (B) applied load, using water as the lubricating fluid. The inset in B shows the typical measurement of the coefficient of friction (data in red) with increasing applied load (data in blue).

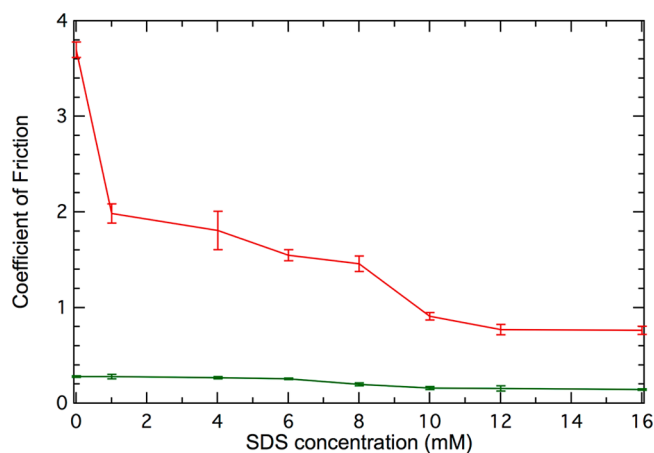


Figure 4. Plot of the coefficient of friction as a function of SDS concentration for a flat surface of PDMS (red line) compared to a textured surface of PDMS (green line). The preload was 45 mN and the shear velocity was maintained at $100 \mu\text{m/s}$.

the probe still makes contact with the textured PDMS surface, which results in a lower coefficient of friction.

Overall, these results show that by creating pores in a compliant polymer surfaces one can exploit hydrodynamic (or mixed) lubrication even at low shear speeds. Low friction can

be maintained for a wide range of shear velocities and applied load. The addition of a boundary lubricant can further reduce friction for a relatively low applied load and shear velocity and it would be interesting to verify whether this effect persists over a wide range of shear velocities and applied loads. Future studies toward optimization of design parameters such as pore density, aspect ratio, polymer stiffness among other important parameters and moving toward biocompatible boundary lubricants could lead to application of such materials in biomedical implants for joint replacement.

■ EXPERIMENTAL SECTION

Conventional photolithography was used to create pillars of Su-8 photoresist (MicroChem) in a square lattice on silicon wafers (Test grade, University wafers). The latter was then used as a mold to obtain the final porous polymer surfaces out of polydimethylmethoxysilane (PDMS) (Sylgard 184, Dow Corning). To facilitate the removal of the PDMS from the mold, we treated the silicon wafers (with Su8 patterns) with Octadecyltrichlorosilane (Sigma-Aldrich). OTS treatment was done by immersing the wafers into a 100 μ L of OTS per 100 mL of pentane (HPLC grade, Pharmaco-Aaper) solution for 5 min. The wafers were then rinsed with pure pentane, DI water, and ethanol to remove excess OTS followed by drying under nitrogen (UHP, Airgas). PDMS was cured for 24 h at 60 °C. A Universal Material Tester (UMT-2, CETR) was used to apply a preload and measure the friction forces between a glass lens (27420, Edmund Optics) with a radius of curvature of 6 mm and the porous PDMS surfaces. To ensure that the surfaces (both the glass lens and the PDMS surfaces) were clean and that water gets inside the inherently hydrophobic PDMS channels, we exposed the samples to an air plasma for 60 s. The porous PDMS surfaces were then submerged in water under vacuum for approximately 20 s to remove the air from the pores and replace it with water. Throughout the experiments, the samples were kept submerged in water to compensate losses due to evaporation. Stock solutions of sodium dodecyl sulfate (Sigma-Aldrich) were made at various concentrations to study the effect of adding a boundary lubricant. All chemicals used were used as-received.

■ ASSOCIATED CONTENT

Supporting Information

The Supporting Information is available free of charge on the ACS Publications website at DOI: 10.1021/acsami.5b05181.

Additional figures and experimental details (PDF)

■ AUTHOR INFORMATION

Corresponding Author

*E-mail: npesika@tulane.edu.

Notes

The authors declare no competing financial interest.

■ ACKNOWLEDGMENTS

This work was supported by NSF grant CMMI-1301286 and by ONR through U.S. Naval Research Laboratory base funds (NRL 6.1 WU#69-4640). The opinions and assertions contained herein are those of the authors and are not to be construed as official or reflecting views of the U.S. Navy, Department of Defense, or U.S. Government.

■ REFERENCES

- (1) Mansot, J. L.; Bercion, Y.; Romana, L.; Martin, J. M. Nanolubrication. *Braz. J. Phys.* **2009**, *39* (1A), 186–197.
- (2) Lin, T. W.; Modafe, A.; Shapiro, B.; Ghodssi, R. Characterization Of Dynamic Friction In Mems-Based Microball bearings. *IEEE Trans. Instrum. Meas.* **2004**, *53* (3), 839–846.

- (3) Shabani, R.; Cho, H. J. Flow Rate Analysis of an Ewod-Based Device: How Important are Wetting-Line Pinning and Velocity Effects? *Microfluid. Nanofluid.* **2013**, *15* (5), 587–597.

- (4) Tadmor, R.; Bahadur, P.; Leh, A.; N'guessan, H. E.; Jaini, R.; Dang, L. Measurement of Lateral Adhesion Forces at The Interface Between A Liquid Drop and A Substrate. *Phys. Rev. Lett.* **2009**, *103* (26), 266101.

- (5) Kujawa, J.; Rozicka, A.; Cerneaux, S.; Kujawski, W. The Influence of Surface Modification on The Physicochemical Properties Of Ceramic Membranes. *Colloids Surf., A* **2014**, *443*, 567–575.

- (6) Amonton, G. On The Resistance Originating in Machines. *Proc. French R. Acad. Sci. A* **1699**, *12*, 206–222.

- (7) Tian, Y.; Pesika, N.; Zeng, H.; Rosenberg, K.; Zhao, B.; McGuiggan, P.; Autumn, K.; Israelachvili, J. Adhesion and Friction In Gecko Toe Attachment and Detachment. *Proc. Natl. Acad. Sci. U. S. A.* **2006**, *103* (51), 19320–19325.

- (8) Kadokawa, J.-i. *Ionic Liquids—New Aspects For The Future*; InTech: Rijeka, Croatia, 2013.

- (9) Israelachvili, J. N. *Intermolecular And Surface Forces*, revised third ed.; Academic Press: New York, 2011.

- (10) Tadmor, R. The London-Van Der Waals Interaction Energy Between Objects of Various Geometries. *J. Phys.: Condens. Matter* **2001**, *13* (9), L195.

- (11) Al-Azizi, A. A.; Eryilmaz, O.; Erdemir, A.; Kim, S. H. Effects Of Nanoscale Surface Texture and Lubricant Molecular Structure on Boundary Lubrication in Liquid. *Langmuir* **2013**, *29* (44), 13419–13426.

- (12) Butt, H.-J.; Kappl, M. *Surface and Interfacial Forces*. John Wiley & Sons: New York, 2009.

- (13) Greene, G. W.; Banquy, X.; Lee, D. W.; Lowrey, D. D.; Yu, J.; Israelachvili, J. N. Adaptive Mechanically Controlled Lubrication Mechanism Found in Articular Joints. *Proc. Natl. Acad. Sci. U. S. A.* **2011**, *108* (13), 5255–5259.

- (14) Greene, G. W.; Zappone, B.; Zhao, B.; Söderman, O.; Topgaard, D.; Rata, G.; Israelachvili, J. N. Changes In Pore Morphology and Fluid Transport in Compressed Articular Cartilage and The Implications for Joint Lubrication. *Biomaterials* **2008**, *29* (33), 4455–4462.

- (15) Bonnevie, E.; Baro, V.; Wang, L.; Burris, D. L. In Situ Studies of Cartilage Microtribology: Roles of Speed and Contact Area. *Tribol. Lett.* **2011**, *41* (1), 83–95.

- (16) Murakami, T.; Higaki, H.; Sawae, Y.; Ohtsuki, N.; Moriyama, S.; Nakanishi, Y. Adaptive Multimode Lubrication in Natural Synovial Joints and Artificial Joints. *Proc. Inst. Mech. Eng., Part H* **1998**, *212* (1), 23–35.

- (17) Greene, G. W.; Olszewska, A.; Osterberg, M.; Zhu, H.; Horn, R. A Cartilage-Inspired Lubrication System. *Soft Matter* **2014**, *10* (2), 374–382.

- (18) Katta, J.; Jin, Z.; Ingham, E.; Fisher, J. Biotribology Of Articular Cartilage—A Review of The Recent Advances. *Medical engineering & physics* **2008**, *30* (10), 1349–1363.

- (19) Poole, A. R.; Kojima, T.; Yasuda, T.; Mwale, F.; Kobayashi, M.; Laverty, S. Composition and Structure of Articular Cartilage: A Template for Tissue Repair. *Clin. Orthop. Relat. Res.* **2001**, *391*, S26–S33.

- (20) Ap Gwynn, I.; Wade, S.; Ito, K.; Richards, R. Novel Aspects to the Structure of Rabbit Articular Cartilage. *Eur. Cell Mater.* **2002**, *4*, 18–29.

- (21) Han, M.-J.; Bhattacharyya, D. Changes in Morphology and Transport Characteristics of Polysulfone Membranes Prepared by Different Demixing Conditions. *J. Membr. Sci.* **1995**, *98* (3), 191–200.

- (22) Katta, J.; Pawaskar, S.; Jin, Z.; Ingham, E.; Fisher, J. Effect of Load Variation On the Friction Properties of Articular Cartilage. *Proc. Inst. Mech. Eng., Part J* **2007**, *221* (3), 175–181.

- (23) Forster, H.; Fisher, J. The Influence of Loading Time and Lubricant On The Friction of Articular Cartilage. *Proc. Inst. Mech. Eng., Part H* **1996**, *210* (2), 109–119.

(24) Maroudas, A.; Bannan, C. Measurement of Swelling Pressure in Cartilage and Comparison With the Osmotic Pressure of Constituent Proteoglycans. *Biorheology* **1980**, *18* (3–6), 619–632.

(25) Soltz, M. A.; Ateshian, G. A. Interstitial Fluid Pressurization During Confined Compression Cyclical Loading of Articular Cartilage. *Ann. Biomed. Eng.* **2000**, *28* (2), 150–159.

(26) Federico, S.; Grillo, A.; La Rosa, G.; Giaquinta, G.; Herzog, W. A Transversely Isotropic, Transversely Homogeneous Microstructural-Statistical Model of Articular Cartilage. *J. Biomech.* **2005**, *38* (10), 2008–2018.

(27) Schmidt, T. A.; Gastelum, N. S.; Nguyen, Q. T.; Schumacher, B. L.; Sah, R. L. Boundary Lubrication of Articular Cartilage: Role of Synovial Fluid Constituents. *Arthritis Rheum.* **2007**, *56* (3), 882–891.

(28) Hong, S. M.; Kim, S. H.; Kim, J. H.; Hwang, H. I. Hydrophilic Surface Modification of PDMS Using Atmospheric Rf Plasma. *J. Phys.: Conf. Ser.* **2006**, *34*, 656.

(29) Lötters, J.; Olthuis, W.; Veltink, P.; Bergveld, P. The Mechanical Properties of the Rubber Elastic Polymer Polydimethylsiloxane for Sensor Applications. *J. Micromech. Microeng.* **1997**, *7* (3), 145.

(30) Gao, J. P.; Luedtke, W. D.; Gourdon, D.; Ruths, M.; Israelachvili, J. N.; Landman, U. Frictional Forces and Amontons' Law: From The Molecular to The Macroscopic Scale. *J. Phys. Chem. B* **2004**, *108* (11), 3410–3425.